Current Biology *17*, 1595–1600, September 18, 2007 DOI 10.1016/j.cub.2007.08.036

Report

UNC-80 and the NCA Ion Channels Contribute to Endocytosis Defects in Synaptojanin Mutants

Maelle Jospin,[1] Shigeki Watanabe,[1,2] Deepa Joshi,[1] Sean Young,[1] Kevin Hamming,[3] Colin Thacker,[3] Terrance P. Snutch,[3] Erik M. Jorgensen,[1,2] and Kim Schuske[1,*]

[1]Department of Biology
[2]Howard Hughes Medical Institute
University of Utah
257 South 1400 East
Salt Lake City, UT 84112-0840
[3]Michael Smith Laboratories
University of British Columbia
Vancouver, British Columbia V6T 1Z3
Canada

Summary

Synaptojanin is a lipid phosphatase required to degrade phosphatidylinositol 4,5 bisphosphate (PIP_2) at cell membranes during synaptic vesicle recycling [1, 2]. Synaptojanin mutants in *C. elegans* are severely uncoordinated and are depleted of synaptic vesicles, possibly because of accumulation of PIP_2 [2]. To identify proteins that act downstream of PIP_2 during endocytosis, we screened for suppressors of synaptojanin mutants in the nematode *C. elegans*. A class of uncoordinated mutants called "fainters" partially suppress the locomotory, vesicle depletion, and electrophysiological defects in synaptojanin mutants. These suppressor loci include the genes for the NCA ion channels [3], which are homologs of the vertebrate cation leak channel NALCN [4], and a novel gene called *unc-80*. We demonstrate that *unc-80* encodes a novel, but highly conserved, neuronal protein required for the proper localization of the NCA-1 and NCA-2 ion channel subunits. These data suggest that activation of the NCA ion channel in synaptojanin mutants leads to defects in recycling of synaptic vesicles.

Results and Discussion

unc-80 Is a Suppressor of Synaptojanin Mutant Uncoordination

Synaptojanin mutants accumulate PIP_2 [1] and have defects in synaptic vesicle endocytosis in mice, flies, and worms [1, 2, 5, 6]. To identify proteins that act downstream of PIP_2 during synaptic vesicle endocytosis, we screened for suppressors of synaptojanin mutants (*unc-26*) in *C. elegans*. In the screen, we identified *ox301*, an allele of the gene *uncoordinated-80 (unc-80)*. To quantify suppression, we performed race assays (Table 1; Figure S1 in the Supplemental Data available online). All three alleles of *unc-80* tested were able to suppress the locomotion defect of *unc-26* mutants (Table 1; Figure S1). In addition, mutations in *unc-80* suppressed both a hypomorphic allele of *unc-26(e314)* and, to a lesser degree, a null allele of *unc-26(s1710)*. Because *unc-80* mutations suppress both weak and null alleles of *unc-26*, it is likely that *unc-80* acts downstream, or in parallel to, synaptojanin.

One possible mechanism for suppression is that *unc*-80 mutants could simply be hyperactive. However, *unc-80* mutants are not hyperactive; in fact, they are somewhat sluggish. *unc-80* mutants can move, but they generally spend their time lying still on the plate. If motivated by a sudden stimulus, animals move two body lengths and abruptly stop, in a phenotype called "fainting." The fainting phenotype is still observed in *unc-26 unc-80* double mutants. Moreover, *unc-80* does not appear to nonspecifically increase neurotransmission, because it is not a general suppressor of synaptic transmission mutants (Table 1). In most cases, no strong genetic interactions were found between *unc-80* and other synaptic transmission mutants. The only consistent effect was that *unc-80* suppressed other mutations involved in PIP_2 metabolism. Endophilin (*unc-57*) binds synaptojanin and localizes it to membranes at synapses [5, 7–10]; perhaps not surprisingly, *unc-80* mutations also suppress the locomotory phenotype of *unc-57* mutants. PIP_2 is synthesized by the type 1 PIP kinase (*ppk-1* in *C. elegans*) [11, 12], and overexpression of PPK-1 causes an uncoordinated phenotype (D. Weinkove, M. Bastiani, and K.S., unpublished data). Again, mutations in *unc-80* suppress the locomotory phenotype of this strain. These data suggest that mutations in *unc-80* may be suppressing defects caused by the accumulation of PIP_2.

unc-80 Encodes a Novel Conserved Protein

The uncoordinated phenotype of the *unc-80* mutation was mapped by single nucleotide polymorphisms to an interval on the right arm of chromosome V [13]. We used RNA interference in an RNAi-sensitized background *(eri-1 lin-15b)* [14] to screen candidate open reading frames for phenocopy of the *unc-80* behavioral defect [15]. We found that F25C8.3 gave a fainter phenotype similar to *unc-80* mutants. To show that F25C8.3 is indeed the *unc-80* locus, we rescued *unc-80* mutants with wild-type F25C8.3 DNA and identified the DNA lesion in six *unc-80* mutant alleles (Figure 1A; Figure S2, Table S1).

UNC-80 is a large protein with at least two isoforms (Figure S2; Wormbase). Domain and motif recognition programs failed to suggest a function for the predicted UNC-80 protein; however, it is highly conserved across its length to single proteins in other metazoans (Figure 1A). Thus, UNC-80 is the founding member of an evolutionarily conserved family of proteins.

unc-80 Is Expressed in Neurons

To determine in which cells *unc-80* is expressed, we placed GFP under the control of the *unc-80* promoter (*Punc-80:GFP*). The *unc-80* GFP reporter is broadly expressed in the nervous system (Figure 1B). The

*Correspondence: schuske@biology.utah.edu

Table 1. Worm Race Locomotion Assay in Double Mutants

	Locus 1				
	Wild-Type	Synaptojanin Hypomorph *unc-26(e314)*	Synaptojanin Null[a] *unc-26(s1710)*	*unc-80 (ox301)*	*nca-2(gk5); nca-1(gk9)*
	99 ± 0.7, n = 3	16 ± 1.9, n = 15	1.2 ± 0.3, n = 13	90 ± 5.2, n = 3	98 ± 0.6, n = 3
Locus 2					
UNC-80: *unc-80(ox301)*	90 ± 5.2, n = 3	69 ± 6.2, n = 4; p < 0.0001	12.3 ± 3.3, n = 3; p < 0.0001		
UNC-79: *unc-79(e1068)*	83 ± 4.0, n = 3	53 ± 8.1, n = 3; p < 0.0001	6.9 ± 1.2, n = 7; p < 0.0001		
NCA channel: *nca-2(gk5); nca-1(gk9)*	98 ± 0.6, n = 3	80 ± 6.3, n = 5; p < 0.0001	12.7 ± 2.3, n = 8; p < 0.0001		
Ca_V2 Ca^{2+} channel: *unc-2(lj1)*	56 ± 3.7, n = 8	0.0, n = 6[b]		43 ± 5.4, n = 6; p = 0.6	
Ryanodine receptor: *unc-68(r1162)*	46 ± 11.2, n = 7	0.24 ± 0.24, n = 5; p = 0.0001		43 ± 12.4, n = 5; p = 0.8	
Ca_V1 Ca^{2+} channel: *egl-19(n582)*	73 ± 4.1, n = 9	4.2 ± 0.96, n = 7; p = 0.0003		15 ± 2.5, n = 5; p < 0.0001	6.1 ± 3.5, n = 4; p < 0.0001
Syntaxin: *unc-64(e246)*	34 ± 4.6, n = 3	0.0, n = 3[b]	0.0, n = 4[b]	51 ± 1.7, n = 3; p = 0.02	
UNC-13: *unc-13(n2318)*	99 ± 0.0, n = 3	12 ± 3.7, n = 5; p = 0.32	0.2 ± 0.1, n = 3; p = 0.11		
Synaptotagmin: *snt-1(e2665)*[a]	1.3 ± 0.9, n = 3			0.3 ± 0.3, n = 3; p = 0.35	
Phospholipase Cβ: *egl-8(sa47)*	69 ± 10.7, n = 3			52 ± 3.7, n = 3; p = 0.2	
AP180: *unc-11(e47)*[a]	16 ± 2.5, n = 4			36 ± 6, n = 4; p = 0.02	
Endophilin: *unc-57(ok310)*[a]	16 ± 3.1, n = 4			46 ± 5.6, n = 4; p = 0.0034	
Type 1 PIP kinase overexpression: *gqIs25[Prab-3;PPK-1]*	17 ± 5.2, n = 5			75 ± 7.2, n = 5; p = 0.0002	

Double and triple mutants were constructed between the genotypes designated "locus 1" and "locus 2." Percent of animals reaching the food ± SEM.
[a] 2 hr assays were used, all others are 1 hr.
[b] Unable to calculate p value because none of the double mutants arrived at the food.

reporter is expressed in both acetylcholine and GABA motor neurons as determined by double-labeling (Figure S3A). Although expression is observed in other tissues (Figure 1B), no expression was observed in the body muscle, suggesting that the uncoordinated phenotype is likely due to a loss of UNC-80 function in neurons.

UNC-80 Is Required for NCA-1 Localization or Stabilization in Axons

Only two other strains exhibit the fainter phenotype: animals lacking both subunits of a novel ion channel family encoded by the *nca-1* and *nca-2* genes [3], and animals lacking a large novel protein encoded by the *unc-79* gene [3, 16]. Fainter mutants have additional phenotypes in common. First, when placed in liquid, they are unable to swim, but instead become rigid and appear to have tremors (J. Pierce-Shimomura, personal communication; Table S1). Second, fainter mutants have altered sensitivity to volatile anesthetics such as halothane and enflurane [3, 16–18]. Third, *unc-79* mutants and *nca-1 nca-2* double mutants suppress the uncoordinated phenotype of animals lacking synaptojanin (Table 1; Figure S1). Together, these data suggest that UNC-80, UNC-79, and the NCA ion channels function in the same pathway.

Like *unc-80*, the *nca* genes are expressed in both excitatory and inhibitory motor neurons (Figures S3B and S3C). Interestingly, the mouse homologs of *unc-80* (C030018G13) and of *nca* (A930012M17) also exhibit coincident expression patterns in the hippocampus, cerebellum, and piriform cortex (http://www.brainatlas.org) [19]. The coexpression and similar mutant phenotypes of the *unc-80* and *nca* genes suggest that these proteins may function together.

To determine whether *unc-80* is required for NCA localization, the distributions of the rescuing NCA-1::GFP and NCA-2::GFP fusion proteins (Table S1) were analyzed in *unc-80* mutants. In control animals, NCA-1::GFP and NCA-2::GFP are diffusely distributed along axons and do not appear to be enriched at synaptic sites (Figures 2A and 2B; Figures S3B, S3C, and S4A). In the absence of *unc-80*, axonal NCA-1::GFP and NCA-2::GFP expression is reduced in the axons of motor neurons (Figure S4A) and nerve ring (Figures 2A and 2B). Compared to wild-type levels, NCA-1::GFP and NCA-2::GFP levels in the nerve ring are reduced to 40% and 48%, respectively (Figure 2C). However, expression in cell bodies is not reduced, and may actually be increased, suggesting that NCA-1::GFP and NCA-2::GFP protein is still made in the absence of *unc-80*. By contrast, axonal fluorescence of the voltage-gated calcium channel (UNC-2::GFP), which is related to the vertebrate Ca_V2 family of synaptic calcium channels, is not affected in *unc-80* mutants (Figure 2C; Figure S4B). Other synaptic components are also properly localized, including the synaptic vesicle proteins synaptobrevin

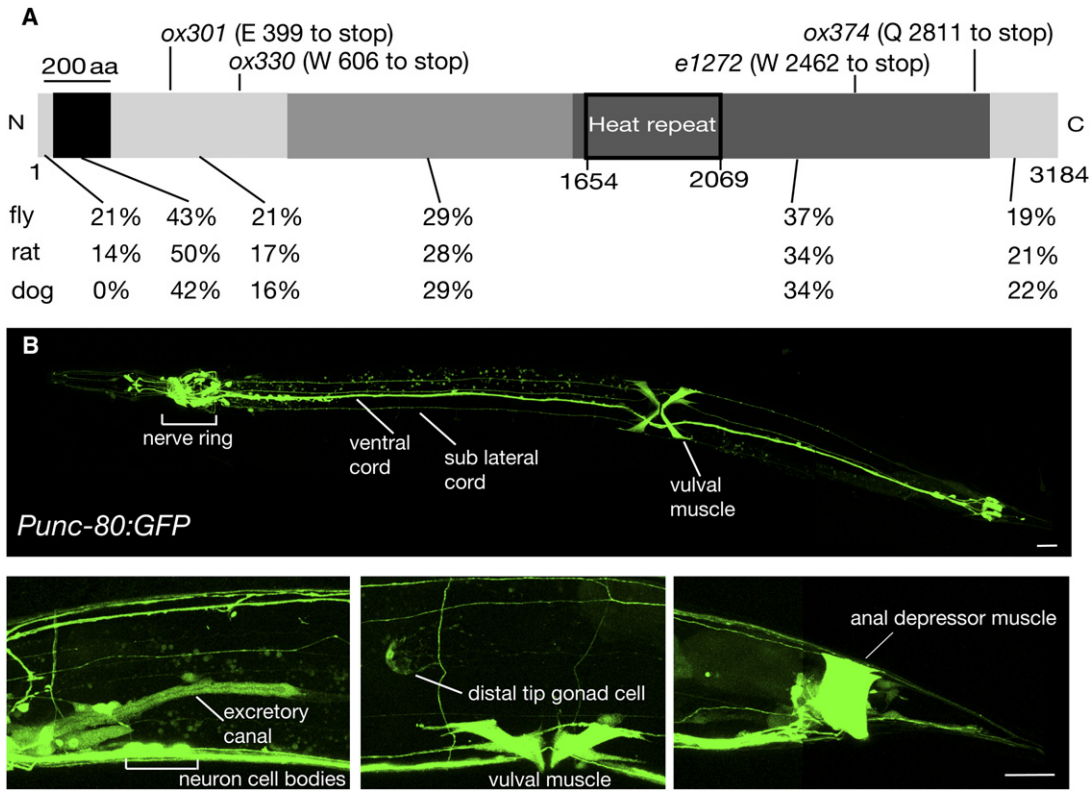

Figure 1. *unc-80* Encodes a Large, Conserved Neuronal Protein

(A) *unc-80* encodes a protein predicted to be 3184 amino acids in length (splice form F25C8.3a). Dark regions indicate strong conservation with homologs in other species. The percent identity between *C. elegans* and homologous proteins in *Drosophila* (CG18437-PA), rat (XP_001053529), and canine (XP_545626) for each of these regions is shown below. Partial sequences for mouse (XP_898856) and human (C2orf21/EAW70465) also exist. A Heat domain was predicted by SMART, with a score of 9 e* −06, but not by other domain search programs including Interpro and Motif scan.

(B) *unc-80* is strongly expressed in neurons. An adult hermaphrodite expressing *Punc-80:GFP* is shown, ventral side is up. Strong expression is observed in the nervous system and in the vulval muscle. Below are magnified images showing expression in the anterior excretory canal just posterior of the head, the vulval muscle, distal tip cell of the gonad, and the anal depressor muscle in the tail, lateral views. Scale bars represent 10 μm.

and synaptotagmin and endocytic sites as marked by clathrin (Figures S4C and S4D). Thus, UNC-80 appears to be required for localization of NCA-1 and NCA-2 in the axon membrane, although we cannot rule out an additional role in channel function.

UNC-80 has a similar function as another protein UNC-79, which is required for maintaining NCA protein expression levels [3]. Therefore, in *C. elegans*, the normal function of the NCA ion channel requires two large proteins (UNC-79 and UNC-80) that contain no clear domains but are strongly conserved in all animals.

Restoration of Synaptic Vesicle Number in the Synaptojanin Mutants

Why does disruption of NCA channel function suppress synaptojanin mutant uncoordination? The most profound synaptic phenotype in *unc-26* mutants is that there are fewer synaptic vesicles [2]. To determine whether *unc-80* and *nca-1 nca-2* mutations suppress the synaptic vesicle depletion of *unc-26* mutants, we characterized the ultrastructure of synapses in these genotypes by a high-pressure freezing protocol. The number of synaptic vesicles in *unc-26(s1710)* mutants was reduced compared to the wild-type (Figure 3A; 42% in acetylcholine neurons and 32% in GABA neurons). The remaining vesicles were often distributed at a distance from the presynaptic density arranged in a "string-of-pearls" (Figure 3B). The string-of-pearls phenotype of *unc-26* mutants was not suppressed by mutations in *unc-80* or *nca-1 nca-2* (Figure 3B). However, synaptic vesicle number in *unc-26 unc-80* double mutants, although still reduced compared to the wild-type (81% in acetylcholine and 60% in GABA neurons; Figure 3A), shows a significant improvement over *unc-26* mutants alone (1.9-fold and 1.8-fold more vesicles, respectively). Similar levels of suppression are observed in *nca-1 nca-2 unc-26* triple mutants (68% synaptic vesicles in acetylcholine neurons and 55% in GABA neurons compared to the wild-type; Figure 3A) but have 1.6-fold more synaptic vesicles in acetylcholine neurons and 1.7-fold more in GABA neurons than *unc-26(s1710)*. The increase in synaptic vesicle number suggests that the recycling defect in *unc-26* mutants is ameliorated by the loss of UNC-80 or NCA proteins.

Even in an otherwise wild-type background, *unc-80* and *nca-1 nca-2* mutants exhibit an increase in synaptic vesicle number at both acetylcholine (1.2-fold in *unc-80* and 1.2-fold in *nca-1; nca-2*) and GABA synapses

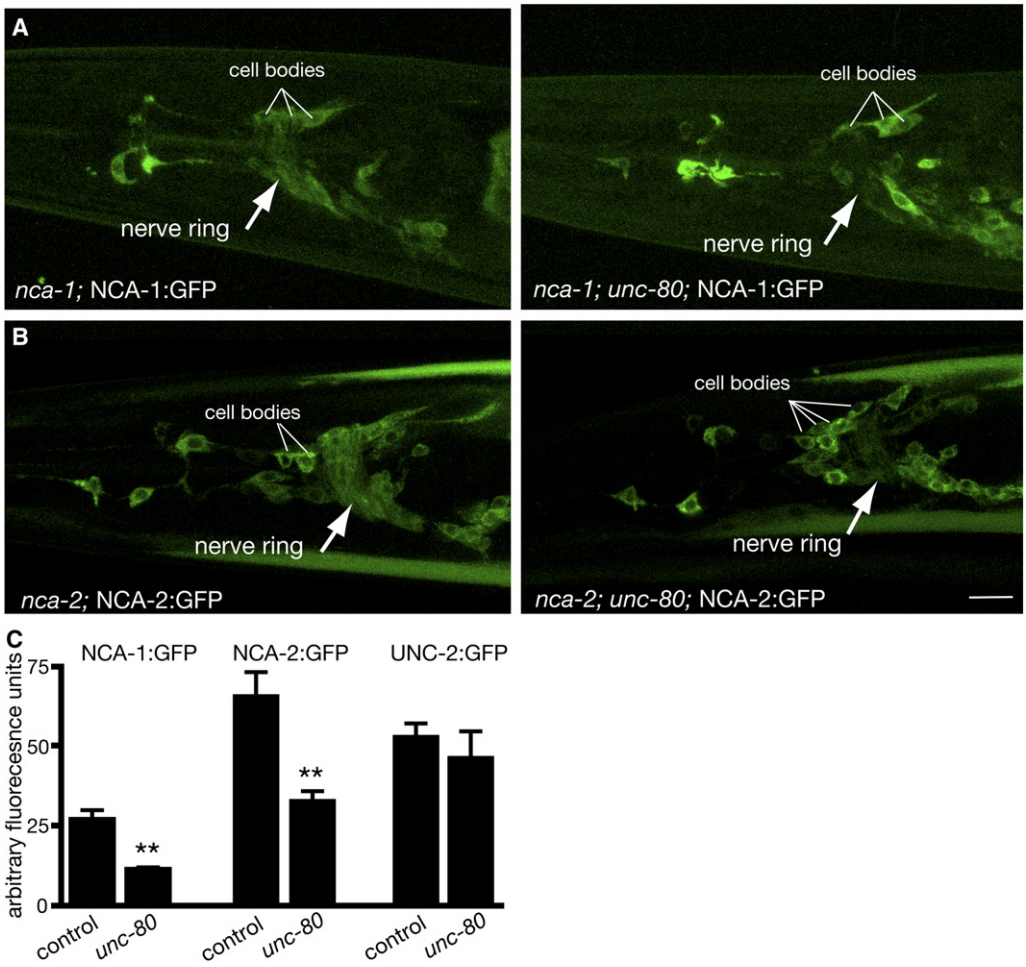

Figure 2. Localization of NCA-1 and NCA-2 Are Disrupted in *unc-80* Mutants

(A) NCA-1:GFP expression in the head of an *nca-1(gk9)* animal (left) and *nca-1(gk9); unc-80(ox301)* mutant (right).

(B) NCA-2:GFP expression in the head of an *nca-2(gk5)* animal (left) and *nca-2(gk5); unc-80(ox301)* mutant (right).

In (A) and (B), ventral is at the top, anterior to the left. Scale bar represents 10 μm.

(C) Quantitative imaging of NCA-1:GFP, NCA-2:GFP, and UNC-2:GFP fluorescence in control and *unc-80(ox301)* animals. The right side of the nerve ring was imaged from the center of the pharynx to the hypodermis. Projected stacks, including the entire right side of the nerve ring, were used for quantification (average fluorescence intensity ± SEM, n = animals): NCA-1:GFP (*vals46*): *nca-1(gk9)*, 25.2 ± 3.3, n = 5; *nca-1(gk9); unc-80(ox301)*, 10.1 ± 0.6, n = 4; p = 0.005, two-tailed, unpaired t test. A similar effect is seen for NCA-1:GFP (*vals46*) in a wild-type background, wild-type: 28.4 ± 3.2, n = 6; *unc-80(ox301)*: 9.7 ± 1.1, n = 6; p = 0.0003. NCA-2:GFP (*vals41*): *nca-2(gk5)*, 64.7 ± 8.0, n = 6; *nca-2(gk5); unc-80(ox301)*, 31.4 ± 3.2, n = 6; p = 0.003. UNC-2:GFP (*vals33*): *unc-2(e55)*, 52.0 ± 4.5, n = 5; *unc-2(e55); unc-80(ox301)*, 44.7 ± 8.7, n = 5; p = 0.48. **p = 0.005–0.001.

(1.5-fold in *unc-80* and 1.2-fold in *nca-1; nca-2*) (Figure 3A). It is possible that *unc-80* and *nca-1 nca-2* suppress the synaptojanin phenotype indirectly; that is, that mutating these genes leads to an increase in synaptic vesicle number in any genotype. However, the proportional change is much greater in the *unc-26* mutant background (Figure 3A), suggesting that the NCA channel function is reducing synaptic vesicle number because of the synaptojanin mutant defect—perhaps because of inappropriate increases in PIP_2.

Restoration of Synaptic Transmission in Synaptojanin Mutants

Do mutations in *unc-80* and *nca-1 nca-2* alleviate the exocytosis defects observed in synaptojanin mutants? We recorded miniature postsynaptic currents ("minis") at neuromuscular junctions by using voltage-clamp recordings from body muscle cells (Figures 3C and 3D). The frequency of minis in synaptojanin null mutants is 17% compared to wild-type animals (0.5 mM calcium). The frequency of minis is increased by more than 2-fold in *unc-26(s1710) unc-80(ox301)* and *nca-1 nca-2 unc-26(s1710)* mutants, suggesting that loss of *unc-80* or *nca-1 nca-2* confers a significant improvement in synaptic transmission in the absence of synaptojanin.

The fainter phenotype observed in *unc-80* and *nca-1 nca-2* mutants suggests that these mutants have a defect in synaptic transmission. In fact, these mutants exhibit a decrease in acetylcholine release as assayed by resistance to an inhibitor of acetylcholinesterase (Figure S5A). A defect in neurotransmission is not so apparent at an electrophysiological level. In low calcium (0.5 mM calcium), mini frequencies are normal in these strains (Figures 3C and 3D). By contrast, in high calcium

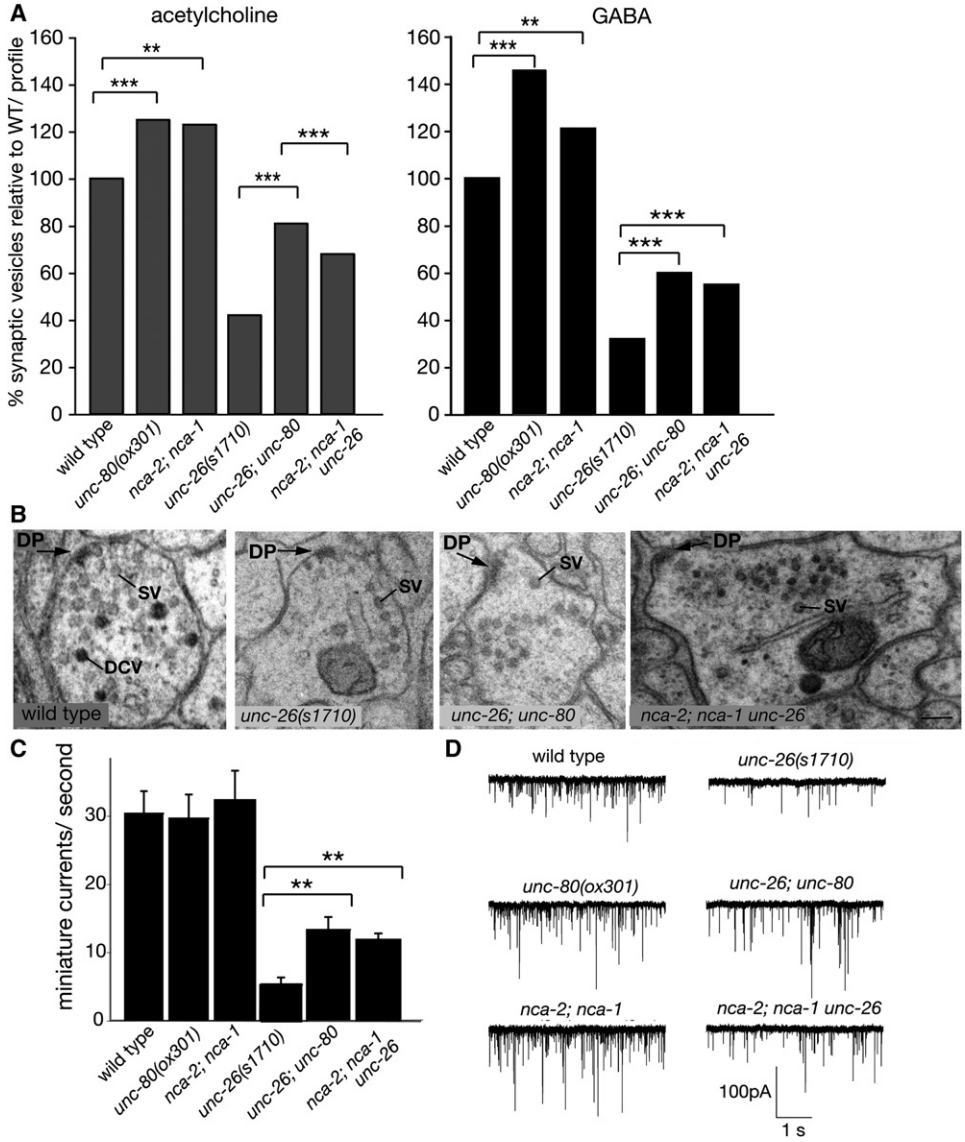

Figure 3. Suppression of Synaptojanin Mutant Phenotypes by *unc-80* and by *nca-1; nca-2*

(A) Vesicle number in mutants. The percent of synaptic vesicles per profile relative to the wild-type is shown. Average numbers of synaptic vesicles per profile were calculated for both acetylcholine and GABA neurons from two young adult hermaphrodites. Left, genotype acetylcholine synapses (number of synaptic vesicles per profile ± SEM, n = synapses): wild-type (20.6 ± 0.9, n = 14), *unc-80* (25.9 ± 1.0, n = 10), *nca-2; nca-1* (25.4 ± 1.4, n = 8), *unc-26(s1710)* (8.9 ± 0.4, n = 19), *unc-26; unc-80* (16.7 ± 1.1, n = 10), *nca-2; nca-1 unc-26* (14.1 ± 1.0, n = 10). Right, genotype GABA synapses (number of synaptic vesicles per profile ± SEM, n = synapses): wild-type (33.8 ± 1.2, n = 13), *unc-80* (49.2 ± 2.3, n = 10), *nca-2; nca-1* (40.8 ± 2.6, n = 10), *unc-26* (10.9 ± 0.6, n = 17), *unc-26; unc-80* (20.1 ± 1.5, n = 10), *nca-2; nca-1 unc-26* (18.6 ± 1.7, n = 10). p value calculated by two-tailed, unpaired t test. **p = 0.005–0.001, ***p < 0.001.

(B) Electron micrographs of profiles from acetylcholine neurons containing a dense projection (DP), arrows; lines indicate synaptic vesicles (SV) and dense core vesicles (DCV). Scale bar represents 100 nm.

(C) Frequency of miniature postsynaptic currents (minis) in the presence of 0.5 mM external calcium. Minis were recorded at a holding potential of −60 mV on ventral medial body muscle cells. Minis per second ± SEM, n = animals: wild-type (30.3 ± 3.2, n = 12), *unc-80* (29.5 ± 3.5, n = 11), *nca-2; nca-1* (32.2 ± 4.3, n = 8), *unc-26(s1710)* (5.7 ± 1.1, n = 7), *unc-26; unc-80* (13.3 ± 1.9, n = 7), *nca-2; nca-1 unc-26* (11.8 ± 1, n = 7). p value calculated by two-tailed, unpaired t test. **p = 0.005–0.001.

(D) Representative traces recorded in 0.5 mM calcium.

(5.0 mM calcium), mini frequencies are more variable than in the wild-type (Figure S5B). Half of the cells exhibited very low mini frequencies (lower than 20 fusions per second) in *unc-80(ox301)*, in *unc-80(ox330)*, and in *nca-1 nca-2*, but not in wild-type animals (Figures S5C and S5D). These data suggest that increased extracellular calcium reduces the rate of synaptic vesicle release in *unc-80* and *nca-1 nca-2* mutants.

Models for *unc-80* and *nca-1 nca-2* Suppression of *unc-26*

How do mutations in *unc-80* and *nca-1 nca-2* suppress the depletion of synaptic vesicles in synaptojanin mutants? One possibility is that these mutations simply reduce exocytosis and thereby allow the crippled endocytic machinery time to catch up. As observed in aldicarb assays, *unc-80* and *nca-1 nca-2* mutants exhibit

a weak defect in exocytosis. If this model were true, then other mutants defective for exocytosis should also suppress *unc-26*. To test this hypothesis, we made double mutants between *unc-26* and mutations in genes that decrease but do not eliminate synaptic vesicle release. Such mutations did not suppress and in most cases exacerbated the synaptojanin mutant phenotype (Table 1), including mutations in the neural calcium channel Ca_V2 (*unc-2*), the "long-lasting" calcium channel Ca_V1 (*egl-19*), the ryanodine receptor (*unc-68*), and weak mutations in syntaxin (*unc-64*) and UNC-13 (*unc-13*). These data suggest that a general decrease in synaptic vesicle exocytosis is not sufficient to suppress *unc-26* uncoordination.

Another possibility is that the NCA channel function inhibits residual endocytosis of synaptic vesicles in *unc-26* mutants. In support of this model, absence of NCA channel function increases synaptic vesicle numbers in synaptojanin mutants. The increase in synaptic vesicles is mirrored by a proportional increase in synaptic vesicle exocytosis in the suppressed strain.

The original goal of this study was to identify proteins that act downstream of PIP_2 accumulation at the synapse. Elimination of the synaptojanin PIP_2 phosphatase or overexpression of the type 1 PIP kinase would be expected to lead to an accumulation of PIP_2, and both strains generate uncoordinated animals. The uncoordinated phenotypes of both of these strains is suppressed by mutations in NCA channel function. Lipids, including PIP_2, regulate the activity of many ion channels [20]. Our data suggest that the NCA channel may be inappropriately activated by PIP_2 and partially contributes to the synaptojanin mutant phenotype. Mislocalization of the NCA channels in *unc-80* mutants, or elimination of the channels themselves, partially alleviate this effect.

Supplemental Data

Five figures, one table, and Experimental Procedures are available at http://www.current-biology.com/cgi/content/full/17/18/1595/DC1/.

Acknowledgments

We would like to thank M. Zhen for the *nca-1 nca-2 unc-80* strain and for sharing unpublished data, P. Morgan for sharing unpublished data, J. Pierce-Shimomura for sharing *unc-80* mapping data, M. Alion for *unc-80(ox330)* and *unc-80(ox329)*, G. Hollopeter for the *Punc-17:mCherry* strain, M. Gu for the GFP-tagged synaptotagmin strain, B. Grant, K. Sato, and M. Gu for the GFP-tagged clathrin strain, the *C. elegans* Genome Center for strains, and W. Davis for critical reading of the manuscript. Additionally, we would like to thank J. Weis, N. Jorgensen, and D. Lewis for technical assistance. The research was funded by grants from the National Institutes of Health (NS48391 to K.S., NS034307 to E.M.J) and from the Lowe Syndrome Association and the Lowe Syndrome Trust to K.S. and E.M.J. E.M.J. is an Investigator of the Howard Hughes Medical Institute, T.P.S. is supported by an operating grant from the Canadian Institutes for Health Research and a Canada Research Chair, and M.J. is supported by a long-term fellowship from Human Frontier Science Program.

Received: May 11, 2007
Revised: August 2, 2007
Accepted: August 7, 2007
Published online: September 6, 2007

References

1. Cremona, O., Di Paolo, G., Wenk, M., Luthi, A., Kim, W.T., Takei, K., Daniell, L., Nemoto, Y., Shears, S.B., Flavell, R.A., et al. (1999). Essential role of phosphoinositide metabolism in synaptic vesicle recycling. Cell *99*, 179–188.
2. Harris, T.W., Hartwieg, E., Horvitz, H.R., and Jorgensen, E.M. (2000). Mutations in synaptojanin disrupt synaptic vesicle recycling. J. Cell Biol. *150*, 589–600.
3. Humphrey, J.A., Hamming, K.S., Thacker, C.M., Scott, R.L., Sedensky, M.M., Snutch, T.P., Morgan, P.G., and Nash, H.A. (2007). A putative cation channel and its novel regulator: cross-species conservation of effects on general anesthesia. Curr. Biol. *17*, 624–629.
4. Lu, B., Su, Y., Das, S., Liu, J., Xia, J., and Ren, D. (2007). The neuronal channel NALCN contributes resting sodium permeability and is required for normal respiratory rhythm. Cell *129*, 371–383.
5. Verstreken, P., Koh, T.W., Schulze, K.L., Zhai, R.G., Hiesinger, P.R., Zhou, Y., Mehta, S.Q., Cao, Y., Roos, J., and Bellen, H.J. (2003). Synaptojanin is recruited by endophilin to promote synaptic vesicle uncoating. Neuron *40*, 733–748.
6. Dickman, D.K., Horne, J.A., Meinertzhagen, I.A., and Schwarz, T.L. (2005). A slowed classical pathway rather than kiss-and-run mediates endocytosis at synapses lacking synaptojanin and endophilin. Cell *123*, 521–533.
7. Schuske, K.R., Richmond, J.E., Matthies, D.S., Davis, W.S., Runz, S., Rube, D.A., van der Bliek, A.M., and Jorgensen, E.M. (2003). Endophilin is required for synaptic vesicle endocytosis by localizing synaptojanin. Neuron *40*, 749–762.
8. Micheva, K.D., Kay, B.K., and McPherson, P.S. (1997). Synaptojanin forms two separate complexes in the nerve terminal. Interactions with endophilin and amphiphysin. J. Biol. Chem. *272*, 27239–27245.
9. Ringstad, N., Nemoto, Y., and De Camilli, P. (1997). The SH3p4/Sh3p8/SH3p13 protein family: binding partners for synaptojanin and dynamin via a Grb2-like Src homology 3 domain. Proc. Natl. Acad. Sci. USA *94*, 8569–8574.
10. de Heuvel, E., Bell, A.W., Ramjaun, A.R., Wong, K., Sossin, W.S., and McPherson, P.S. (1997). Identification of the major synaptojanin-binding proteins in the brain. J. Biol. Chem. *272*, 8710–8716.
11. Ishihara, H., Shibasaki, Y., Kizuki, N., Katagiri, H., Yazaki, Y., Asano, T., and Oka, Y. (1996). Cloning of cDNAs encoding two isoforms of 68-kDa type I phosphatidylinositol-4-phosphate 5-kinase. J. Biol. Chem. *271*, 23611–23614.
12. Loijens, J.C., and Anderson, R.A. (1996). Type I phosphatidylinositol-4-phosphate 5-kinases are distinct members of this novel lipid kinase family. J. Biol. Chem. *271*, 32937–32943.
13. Davis, M.W., Hammarlund, M., Harrach, T., Hullett, P., Olsen, S., and Jorgensen, E.M. (2005). Rapid single nucleotide polymorphism mapping in *C. elegans*. BMC Genomics *6*, 118.
14. Wang, D., Kennedy, S., Conte, D., Jr., Kim, J.K., Gabel, H.W., Kamath, R.S., Mello, C.C., and Ruvkun, G. (2005). Somatic misexpression of germline P granules and enhanced RNA interference in retinoblastoma pathway mutants. Nature *436*, 593–597.
15. Kamath, R.S., Fraser, A.G., Dong, Y., Poulin, G., Durbin, R., Gotta, M., Kanapin, A., Le Bot, N., Moreno, S., Sohrmann, M., et al. (2003). Systematic functional analysis of the *Caenorhabditis elegans* genome using RNAi. Nature *421*, 231–237.
16. Sedensky, M.M., and Meneely, P.M. (1987). Genetic analysis of halothane sensitivity in *Caenorhabditis elegans*. Science *236*, 952–954.
17. Morgan, P.G., Sedensky, M.M., Meneely, P.M., and Cascorbi, H.F. (1988). The effect of two genes on anesthetic response in the nematode *Caenorhabditis elegans*. Anesthesiology *69*, 246–251.
18. Morgan, P.G., Sedensky, M., and Meneely, P.M. (1990). Multiple sites of action of volatile anesthetics in *Caenorhabditis elegans*. Proc. Natl. Acad. Sci. USA *87*, 2965–2969.
19. Lein, E.S., Hawrylycz, M.J., Ao, N., Ayres, M., Bensinger, A., Bernard, A., Boe, A.F., Boguski, M.S., Brockway, K.S., Byrnes, E.J., et al. (2007). Genome-wide atlas of gene expression in the adult mouse brain. Nature *445*, 168–176.
20. Suh, B.C., and Hille, B. (2005). Regulation of ion channels by phosphatidylinositol 4,5-bisphosphate. Curr. Opin. Neurobiol. *15*, 370–378.